Lattice U(1) gauge model in 3+1 dimensions

C. J. Hamer and M. Aydin
School of Physics, University of New South Wales, P.O. Box 1, Kensington 2033, Australia
(Received 21 December 1990)

The stochastic truncation method has been used to calculate the ground-state energy and string tension for the compact lattice U(1) gauge model in 3+1 dimensions. Finite-size behavior characteristic of a line of fixed points at weak coupling is clearly evident. No sign is seen of a first-order transition at the end point of the critical line: the data seem most consistent with a normal second-order transition.

I. INTRODUCTION

The phase structure of compact lattice U(1) gauge theory is well known.[1-3] At large couplings g the system is in a confining phase, because of the effect of unbound magnetic monopoles (or monopole loops) which produce a dual Meissner effect, confining the electric field lines to very thin "flux tubes." For small couplings, on the other hand, the monopoles are tightly bound together, and the system is in a Coulombic phase with massless photons, giving rise to a line of fixed points. The existence of these two phases has been rigorously proven;[4,5] and the crucial importance of the monopoles has been nicely demonstrated by Barber, Schrock, and Schrader,[6] who showed that if the monopoles are eliminated there is no sign of any phase transition.

The nature of the transition between the weak-coupling and strong-coupling phases has been much less well established. It was originally thought that it might be a Kosterlitz-Thouless transition,[7] by analogy with the O(2) spin model in two dimensions, where topological vortices play a similar role to that of the monopoles above. A number of early Monte Carlo studies[8-13] claimed, however, that the simple model with a Wilson action in fact undergoes an ordinary second-order transition. Jersak and co-workers[14,15] then observed a small, sharp hysteresis effect in the "mean plaquette value," indicating a weak first-order transition, instead—although the discontinuity (if any) in the string tension was too small to measure. Gupta, Novotny, and Cordery[16] and Grösch *et al.*[17] cast some doubt on this result, noting the presence of monopole loops which span the finite lattice, and may explain the hysteresis as a finite-size effect. Subsequently, there have been several Monte Carlo renormalization-group studies. Burkitt[18] and Lang[19] seem to lean towards a second-order transition; while Hasenfratz,[20] using a new interpretation of the expected behavior near a first-order transition, finds the transition is first order. Finally, a precision study by Azcoiti, Di-Carlo, and Grillo[21] finds that the finite-size scaling behavior of the specific heat looks most consistent with a second-order transition. The question has hardly been settled conclusively, even yet.

Studies of the Hamiltonian version of the model have been few and far between. Kogut, Sinclair, and Susskind[22] obtained the first strong-coupling series, and noted evidence of a phase transition. A real-space renormalization-group study by Hamber,[23] and a variational analysis by Heys and Stump,[24] also saw a phase transition but could not determine its order. Monte Carlo calculations have been done by Heys and Stump,[25] and by Chin, Negele, and Koonin[26] and Koonin, Umland, and Zirnbauer[27] used a guided random walk Monte Carlo method to estimate the ground-state energy and its first derivative. Irving and Hamer[28] extended the strong-coupling series, and generated "exact linked cluster expansions" (ELCE's) which seemed to indicate a second-order transition. Some estimates of the ground-state energy have also been obtained by Choe, Duncan, and Roskies[29] using a very interesting Lanczos variational technique, but unfortunately those results are too deep in the weak-coupling regime to be relevant here.

In the present work we apply the stochastic truncation Monte Carlo technique[30,31] to the Hamiltonian model, and determine the ground-state energy and the string tension. The string tension results seem quite reliable, and match nicely to the asymptotic values expected in the weak-coupling limit. There is clear evidence of the expected fixed-point behavior at weak couplings. There is no evidence for a first-order phase transition at the end point of the critical line, and the data seem quite consistent with an ordinary second-order transition, with parameters

$$x^*=0.675\pm0.025, \quad \mu=0.4\pm0.1 \; . \tag{1.1}$$

II. METHOD

The quantum Hamiltonian of the compact U(1) lattice gauge theory can be taken as[32,33] (ignoring an overall multiplicative constant)

$$H=\sum_l L_l^2 - x \sum_p (Z_p+Z_p^\dagger) \; , \tag{2.1}$$

where l denotes links and p denotes plaquettes of the three-dimensional spatial lattice, and the strong-coupling parameter $x=1/g^4$, where g is the bare electric charge. We shall work in a strong-coupling basis in which the

electric flux operator L_l on each link is diagonal, and has the usual integer spectrum of eigenvalues:

$$L_l|i\rangle = n_l|i\rangle, \quad n_l = 0, \pm 1, \pm 2, \ldots . \tag{2.2}$$

The magnetic or plaquette operator Z_p then raises or lowers the electric flux on the four links of the plaquette p by one unit, by virtue of its commutation relations with the L_l:

$$[L_l, Z_p] = \begin{cases} Z_p & \text{if } l \text{ is link 1 or 2 of } p \ , \\ -Z_p & \text{if } l \text{ is link 3 or 4 of } p \ , \\ 0 & \text{otherwise} \ . \end{cases} \tag{2.3}$$

The stochastic truncation method which we have used to treat this model has been discussed in detail elsewhere,[30,31,34,35] and we shall give no more than a summary here. It is a Monte Carlo version of the simple power method for finding the dominant eigenvalue and eigenvector of a matrix. At the mth iteration, the (unnormalized) approximate eigenvector is represented by a superposition of basis states:

$$|\psi^{(m)}\rangle = \sum_i n_i^{(m)}|i\rangle \ , \tag{2.4}$$

where the amplitudes or "occupation numbers" $n_i^{(m)}$ are integers. Define also an "ensemble size"

$$N^{(m)} = \sum_i n_i^{(m)} \tag{2.5}$$

and a "score" $S^{(m)}$ which approximates the eigenvalue; then the trial vector at the next iteration is defined by the rules

$$n_k^{(m+1)} = \sum_i R\left[\frac{H_{ki} n_i^{(m)}}{S^{(m)}}\right] \tag{2.6}$$

and

$$S^{(m+1)} = \frac{N^{(m+1)}}{N^{(m)}} S^{(m)} \ , \tag{2.7}$$

where $R(x)$ is a "rounding function" which rounds x either up or down to the next integer value by a Monte Carlo process such that on average

$$R(x) = x \ . \tag{2.8}$$

Each iteration thus corresponds to a further application of the Hamiltonian matrix to the previous trial vector. When the system reaches equilibrium, a comparison of Eq. (2.6) with the eigenvalue equation shows that, on average,

$$\langle n_k \rangle \propto c_k^0 \tag{2.9}$$

where c_k^0 is the basis-state amplitude in the exact eigenvector, and

$$\langle S \rangle = E_0 \ , \tag{2.10}$$

the corresponding dominant eigenvalue which we are interested in.

Some form of variational guidance is essential in a large system.[26,31] This is implemented in an unbiased fashion by a similarity transformation[35]

$$|\psi'\rangle = U|\psi\rangle \ , \tag{2.11}$$

$$H' = UHU^{-1} \ , \tag{2.12}$$

where we choose

$$U_{ij} = e^{-cE_i^0}\delta_{ij} \tag{2.13}$$

which corresponds to an exponential cutoff on the "unperturbed" energy E_i^0, i.e., the eigenvalue of the electric field term in (2.1) for the basis state $|i\rangle$. The eigenvalues are unchanged by this procedure, but the accuracy of the Monte Carlo estimates may be much improved.

Next, one must arrange for the ground state to be the dominant eigenvector. For the U(1) model, which has an infinite spectrum, this necessitates a cutoff: we chose to discard all basis states such that

$$E_i^0 \geq N_{\text{cut}} \ , \tag{2.14}$$

where N_{cut} is an arbitrary cutoff value, and then define

$$H' = N_{\text{cut}} - H \ . \tag{2.15}$$

The ground state of H should then be the dominant eigenstate (with largest eigenvalue) of H', and furthermore the matrix H' has all elements positive semidefinite. The cutoff (2.14) introduces a systematic error into the result, but N_{cut} was taken sufficiently high ($N_{\text{cut}} = 250$ for the 5×5 lattice) that any such error appeared to be negligible in comparison with the random errors.

The basis states were coded allowing five bits for the electric flux on each link, or a total of 75 words for each complete state on the 5×5 lattice. The computational processing of each state was kept as simple as possible to save processor time. The trial vector was treated as an "ensemble" of $N^{(m)}$ states, each of which was evolved independently; no "gathering" of identical states was performed, nor any symmetrization. The off-diagonal matrix elements were treated by an efficient procedure discussed previously,[31] and all operations were vectorized where possible, so that CPU processing speeds of 10μ sec/state/iteration were achieved for the 5×5 lattice on a Fujitsu VP100 machine.

At each value of the coupling x, a few trial runs were made to select the best value of the variational parameter c, giving as far as possible a stable value for the eigenvalue, with minimum error. Production runs were then carried out of 10^4 iterations, with an initial ensemble size $N^{(0)} = 6\times10^3$; the first 10^3 iterations were discarded, to allow time for equilibration. In the range $0.6 \leq x \leq 0.65$, longer runs of 2×10^4 iterations, with $N^{(0)} = 1.2\times10^4$, were carried out. The statistical error in the result was estimated by "blocking" the data,[36] up to block sizes of 256 iterations, or 1025 iterations for the longer runs. Eigenvalues have been calculated for lattices of M^3 sites with $M = 2$, 3, 4, and 5, assuming periodic boundary conditions.

TABLE I. Table of values for the ground-state energy per site $-E_0/M^3$ as a function of coupling x and lattice size M. Also listed are the resulting estimates of the bulk limit, $M \to \infty$; and estimates from the [2/2] Padé approximant to the strong-coupling series of Irving and Hamer (Ref. 28).

x	$M2$	3	4	5	∞ (est.)	Series
0.2	0.0605(4)	0.0597(3)	0.0600(3)	0.0600(3)	0.0599(3)	0.05999
0.4	0.255(1)	0.2411(3)	0.2406(5)	0.2398(5)	0.2400(5)	0.241(1)
0.5	0.421(1)	0.377(1)	0.377(1)	0.375(1)	0.376(1)	0.379(4)
0.6	0.656(1)	0.557(1)	0.551(1)	0.531(3)	0.54(1)	0.55(1)
0.625	0.725(1)	0.609(1)	0.598(1)	0.574(3)	0.58(1)	
0.65	0.795(1)	0.668(1)	0.652(2)	0.636(2)	0.63(1)	
0.7	0.945(1)	0.804(1)	0.783(2)	0.776(2)	0.77(1)	0.77(4)
0.75	1.103(1)	0.953(1)	0.932(1)	0.923(2)	0.92(1)	
0.8	1.271(1)	1.110(1)	1.087(1)	1.078(1)	1.08(1)	1.03(7)

III. RESULTS

Values for the ground-state energy per site E_0/M^3 are given in Table I and Fig. 1. For comparison, the [2/2] Padé approximant to the strong-coupling series of Irving and Hamer[28] is also shown, together with the weak-coupling asymptotic series[7] (see Appendix A):

$$E_0/M^3 \underset{x\to\infty}{\sim} -6x+4.755x^{1/2}-0.535 , \tag{3.1}$$

where the third (constant) term has been adjusted to fit the data. It can be seen that the Monte Carlo results converge very well to the series estimates in the strong-coupling region; while at weaker couplings (larger x) they appear to be matching on quite well to the asymptotic curve (3.1). Koonin, Umland, and Zirnbauer[27] obtained a result for the 4^3 lattice at $x=0.6$ corresponding to $E_0/M^3=-0.546(6)$ in our terms, which is in excellent agreement with the result in Table I.

The slope of the ground-state energy, $(1/M^3)(dE_0/dx)$, is shown in Fig. 2. This can be found as a ground-state expectation value, using the Feynman-Hellmann theorem, or else by simply taking the slope between neighboring values in Table I. The latter technique seems more accurate, in fact, and was the method we adopted. Here one sees a small steplike structure building up around $x \cong 0.65$, which indicates a probable phase transition; but it is impossible to tell from these data whether the bulk derivative will be continuous, as in a second-order transition, or develop a small step discontinuity (i.e., a "latent heat") as in a first-order transition. Chin, Negele, and Koonin[26] also saw a kink in this derivative, but at somewhat higher value of x, around $x \cong 0.95$. Perhaps this was due to some variational bias in their calculation.

Finally, results for the axial string tension are shown in Table II and Fig. 3, obtained via the formula

$$T=\frac{1}{M}(E_s-E_0) , \tag{3.2}$$

where E_s is the energy of the lowest state in the "string" sector, with a string of unit electric flux along one axis.

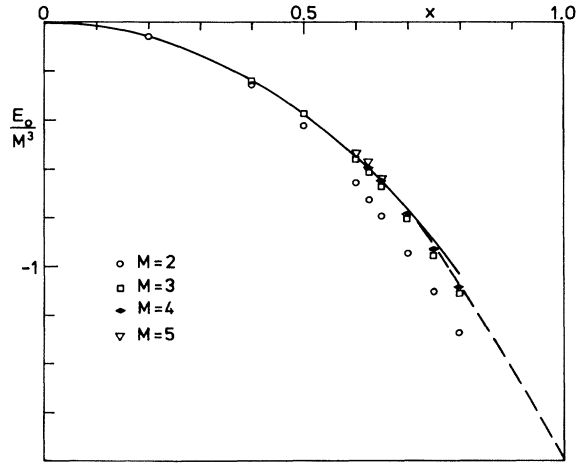

FIG. 1. The ground-state energy per site, E_0/M^3 as a function of x. Monte Carlo results are shown for lattice sizes $M=2$, 3, 4, and 5. The solid line is the [2/2] Padé approximant to the strong-coupling series (Ref. 28), and the dashed line is the weak-coupling series approximation (Ref. 37).

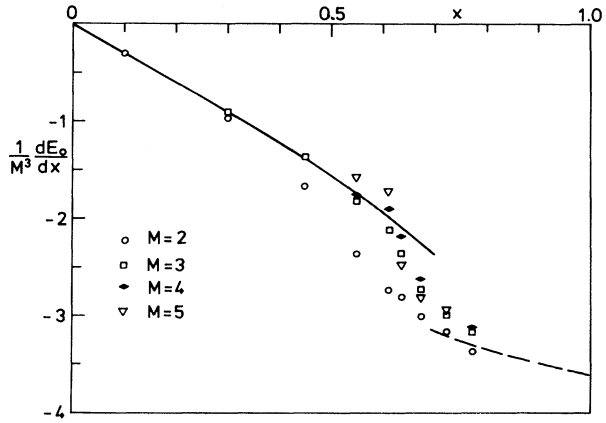

FIG. 2. The derivative of the ground-state energy per site, $(1/M^3)(dE_0/dx)$, as a function of x. Monte Carlo results are shown as in Fig. 1. The solid line is the strong-coupling Padé approximant, and the dashed line is the weak-coupling series.

TABLE II. Table of values for the axial string tension T, as a function of coupling x and lattice size M. Also listed are the resulting estimates of the bulk limit $M \to \infty$ together with estimates from the [2/2] Padé approximant to the strong-coupling series (Ref. 28).

x	$M2$	3	4	5	∞ (est.)	Series
0.2	0.901(3)	0.956(5)	0.97(1)	0.98(1)	0.98(1)	0.9723
0.4	0.634(7)	0.79(1)	0.83(2)	0.87(2)	0.86(3)	0.87(1)
0.5	0.458(7)	0.61(1)	0.68(2)	0.74(4)	0.78(5)	0.75(5)
0.6	0.348(3)	0.36(1)	0.44(3)	0.48(7)	0.6(1)	
0.625	0.325(3)	0.27(1)	0.31(3)	0.12(7)		
0.65	0.310(3)	0.20(1)	0.22(3)	0.02(5)		
0.7	0.30(1)	0.14(1)	0.08(4)	0.12(6)		
0.75	0.28(1)	0.12(1)	0.11(2)	0.08(6)		
0.8	0.28(1)	0.11(2)	0.05(3)	−0.02(4)		

By taking a difference between two large numbers in Eq. (3.2) one inevitably incurs a substantial error, but we know of no more accurate procedure. Also shown for comparison is the [2/2] Padé approximant to the strong-coupling series.[28] The axial string tension is known[32,28] to undergo a "roughening" transition at $x_R \cong 0.56$, however, and the series is of no use beyond that point. It can be seen that the Monte Carlo results seem to converge to the series estimates, within errors, for $x \leq 0.5$.

The finite-size behavior of the Monte Carlo results in Fig. 3 shows two interesting features:

(a) Beyond $x \cong 0.7$, the string tension appears to be leveling off at a constant value for each lattice size M, with the constant value scaling rapidly down toward zero as M increases. A weak-coupling analysis given in Appendix A shows that in fact the finite-lattice values have the asymptotic behavior

$$T(x,M) \underset{x\to\infty}{\sim} \frac{1}{M^2} \tag{3.3}$$

which is in excellent agreement with the numerical results. Now a finite-size scaling behavior $T(x,M) \propto 1/M^2$ for the string tension is characteristic of a critical point (see Ref. 28 and Appendix B); so the finite-size behavior discussed above is evidence of the expected line of fixed points, running from $x \cong 0.7$ to ∞. A very similar phenomenon occurs[38,39] for the mass gap of the O(2) Heisenberg spin model in 1+1 dimensions.

A further demonstration of the line of fixed points is given in Fig. 4, which plots the "scaled string tension ratio"

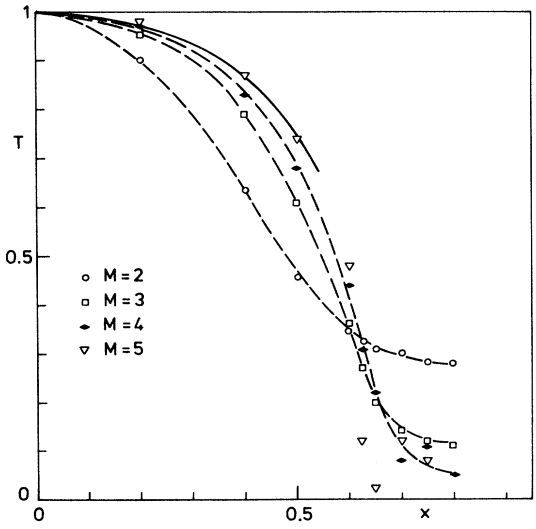

FIG. 3. The axial string tension as a function of x. Monte Carlo results for $M=2$, 3, and 4 are connected by dashed lines to guide the eye. The solid line is the [2/2] Padé approximant to the strong-coupling series (Ref. 28). No error bars are shown.

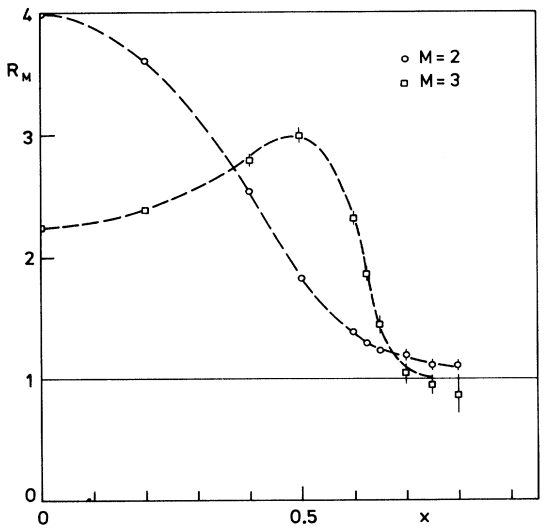

FIG. 4. The scaled string tension ratios R_M as functions of x. Only results for $M=2$ and 3 are shown. The critical value $R_M=1$ is marked with a solid line; the dashed lines are merely to guide the eye.

$$R_M(x)=\frac{M^2T(x,M)}{(M-1)^2T(x,M-1)} \tag{3.4}$$

as a function of x for $M=2$ and 3. At a critical point, we expect $R_M \to 1$. It can be seen that $R_M(x)$ tends very rapidly to the critical value $R_M=1$ for $x \geq 0.7$. The values for $M=4$ and 5 are not accurate enough to be worth plotting, but are entirely consistent with this conclusion.

(b) At smaller x, the string tensions show a "crossover" pattern, scaling upwards to their asymptotic limit at small x, and downwards at large x. At first sight, one might expect this to lead to the development of a step discontinuity in the bulk limit, characteristic of a first-order transition. But a counterexample to this scenario is provided by the Z_2 gauge model in $2+1$ dimensions which is dual to the Ising model and undergoes a second-order transition, and yet displays a similar "crossover" pattern in the finite-lattice results.[30]

To obtain further information on the phase transition, we have calculated the Roomany-Wyld approximant[38] to the Callan-Symanzik β function for the string tension, defined by

$$\frac{\beta(g)}{g}=\frac{\ln[R_M(x)]}{\ln(M/M-1)}\Big/2\left[1-x\frac{\partial}{\partial x}\ln[T(x,M)T(x,M-1)]\right] \tag{3.5}$$

(see Appendix B). Near a second-order critical point, the β function behaves as

$$\frac{\beta(g)}{g} \underset{x\to x^*}{\sim} \frac{x^*-x}{2\mu x^*} \tag{3.6}$$

so that the slope of the β function at the critical point gives the critical index μ. Some results for the smaller lattice sizes, estimated from the values in Table II, are graphed in Fig. 5. We make the following remarks.

(i) As usual for the Roomany-Wyld estimates, which have already incorporated some finite-size scaling, the convergence as M increases is swift. This is illustrated by the closeness of the $M=3$ results and some representative $M=4$ points. The $M=5$ results are consistent with this statement, but are not accurate enough to be worth plotting.

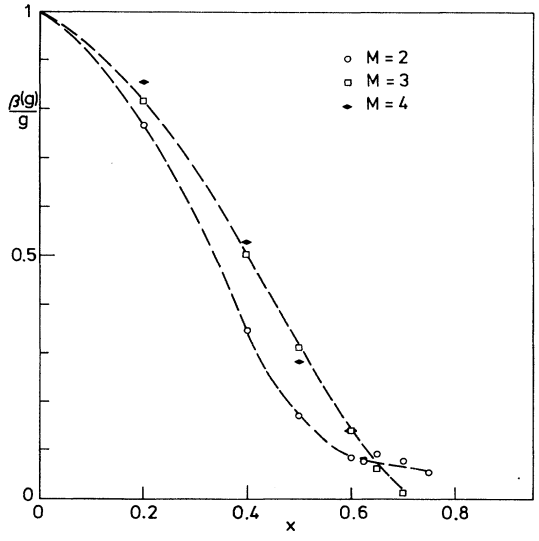

FIG. 5. Graph of the Roomany-Wyld β function $\beta(g)/g$ for the string tension. Results are shown for $M=2$ and 3, together with a few points for $M=4$. Dashed lines are merely to guide the eye. No error bars are shown.

(ii) There is no evidence that the β function will get steeper and steeper near the transition point, and eventually come in vertically, as in a first-order phase transition ("$\mu=0$").

(iii) Fitting an approximate straight line to the data in the range $0.4 \leq x \leq 0.6$ would indicate a second-order phase transition at

$$x^*=0.675\pm0.025 \tag{3.7}$$

with index

$$\mu=0.4\pm0.1\ . \tag{3.8}$$

This position is consistent with the value $x^*=0.72\pm0.08$ obtained by Irving and Hamer[28] from their ELCE analysis, but the index is somewhat lower than their value $\mu=0.65\pm0.12$, or the Euclidean estimates $\mu=0.56(4)$ by DeGrand and Toussaint,[11] 0.78(10) by Bhanot,[10] and 0.75(3) by Caldi.[13] This discrepancy might easily be explained if the critical point were a little further out, and the β function flattened out a little at the foot beyond $x=0.6$.

(iv) We cannot rule out the possibility that the β function may suddenly flatten out right at the foot to an algebraic zero, $\beta(g)/g \sim (x^*-x)^{1+\sigma}$, as in a Kosterlitz-Thouless transition, but there is no particular indication of that in the data.

It would be useful (as always) to have more accurate data, for larger lattices, in the vicinity of the critical point in order to resolve some of these issues with more certainty.

IV. SUMMARY

The stochastic truncation method has been used to obtain finite-lattice estimates of the ground-state energy and string tension for the compact U(1) gauge theory in $3+1$ dimensions. This represents the first time that reliable Monte Carlo estimates have been obtained for the string tension in the Hamiltonian model, as far as we are aware.

The results show very clearly the finite-size scaling behavior characteristic of a line of fixed points beyond $x \cong 0.7$, and match on very nicely to the analytic values expected in the weak-coupling limit.

There is no sign of a first-order phase transition. The finite-lattice string tensions follow a "crossover" pattern, but this seems to be typical of the axial string tension in any model,[30,31] and does not necessarily indicate a first-order transition. The Roomany-Wyld β function appears to vanish linearly as in a normal second-order phase transition, with parameters

$$x^* = 0.675 \pm 0.025, \quad \mu = 0.4 \pm 0.1 \ . \tag{4.1}$$

This estimate of the critical point is consistent with the ELCE result[28] $x^* = 0.72(8)$, but the index value is somewhat lower than other estimates ($\mu \simeq 0.7$).

Of course, one cannot rule out with certainty the possibility of a first-order transition on the one hand, or a Kosterlitz-Thouless transition on the other, because the string tension might always undergo a very small discontinuity, or else a flattening out, very near the foot where data of finite accuracy cannot distinguish it. The data obtained here, however, seem most consistent with an ordinary second-order transition. In any case, the stochastic truncation method seems to have given reasonably reliable and unbiased results, and we hope to apply it to other models.

ACKNOWLEDGMENTS

We are grateful to the Australian National University Supercomputer Facility for a grant of time on their Fujitsu VP100 computer.

APPENDIX A: WEAK-COUPLING ANALYSIS

In this appendix, we shall analyze the weak-coupling behavior of the ground-state energy and string tension following Drell *et al.*,[3] Höfsass and Horsley,[37] and Hamer and Barber.[39]

The U(1) model Hamiltonian can be written

$$H = \sum_l L_l^2 - 2x \sum_p \cos\theta_p \ , \tag{A1}$$

where θ_p is the "plaquette angle" variable associated with each plaquette of the lattice. In the weak-coupling region let $L_l \to -i\partial/\partial\theta_l$, and approximate

$$H \simeq -\sum_l \frac{\partial^2}{\theta_l^2} - 2xN_p + x\sum_p \theta_p^2 \ , \tag{A2}$$

where N_p is the number of plaquettes. The last term can be written as a quadratic form in the "link angles" $\theta(\mathbf{n},\hat{\mathbf{i}})$, where we now denote each link by its origin $\mathbf{n}$ and direction $\hat{\mathbf{i}}$:

$$\sum_p \theta_p^2 = \sum_{\mathbf{m},\mathbf{n},\hat{\mathbf{i}},\hat{\mathbf{j}}} \theta(\mathbf{m},\hat{\mathbf{i}}) D_{ij}(\mathbf{m},\mathbf{n}) \theta(\mathbf{n},\hat{\mathbf{j}}) \equiv \theta^T D \theta \tag{A3}$$

where

$$D_{ij}(\mathbf{m},\mathbf{n}) = \Delta_i \bar{\Delta}_j - \delta_{ij} \sum_k \Delta_k \bar{\Delta}_k \tag{A4}$$

and

$$\Delta_k(\mathbf{m},\mathbf{n}) = \delta_{\mathbf{m}+\hat{\mathbf{k}},\mathbf{n}} - \delta_{\mathbf{m},\mathbf{n}}, \quad \bar{\Delta}_k(\mathbf{m},\mathbf{n}) = \delta_{\mathbf{m},\mathbf{n}} - \delta_{\mathbf{m},\mathbf{n}+\hat{\mathbf{k}}} \tag{A5}$$

are finite-difference operators. Equation (A2) is the Hamiltonian of a generalized simple harmonic oscillator.

The ground-state wave function is a Gaussian

$$|\psi_0\rangle = -\frac{x^{1/2}}{2} \theta^T D^{1/2} \theta \tag{A6}$$

involving a matrix quadratic form in the link angle variables. The corresponding asymptotic expansion for the ground-state energy is

$$E_0 \underset{x\to\infty}{\sim} -2xN_p + x^{1/2}\mathrm{Tr}(D^{1/2}) \ . \tag{A7}$$

The matrix D may be diagonalized by first performing a Fourier transform,

$$\theta(\mathbf{m},\hat{\mathbf{i}}) = \frac{1}{N^{1/2}} \sum_{\mathbf{k}} \tilde{\theta}(\mathbf{k},\hat{\mathbf{i}}) \exp(2\pi i \mathbf{k}\cdot\mathbf{m}) \ , \tag{A8a}$$

$$\tilde{\theta}(\mathbf{k},\hat{\mathbf{i}}) = \frac{1}{N^{1/2}} \sum_{\mathbf{m}} \theta(\mathbf{m},\hat{\mathbf{i}}) \exp(-2\pi i \mathbf{k}\cdot\mathbf{m}) \ , \tag{A8b}$$

where N is the number of lattice sites, and then diagonalizing in the subspace of directions $\hat{\mathbf{i}}$. The result in three space dimensions is

$$\mathrm{Tr}D^{1/2} = 2\sum_{\mathbf{k}} \left[2\sum_{\hat{\mathbf{i}}} (1-\cos 2\pi k_i) \right]^{1/2} \tag{A9}$$

$$\underset{N\to\infty}{\sim} 2\frac{N}{(2\pi)^3} \int_{-\pi}^{\pi} d^3p \left[2\sum_{\hat{\mathbf{i}}} (1-\cos p_i) \right]^{1/2} \tag{A10}$$

$$= 4.755N \tag{A11}$$

according to Höfsass and Horsley.[37] Thus from (A7),

$$E_0/M^3 \underset{x\to\infty}{\sim} -6x + 4.755x^{1/2} \ . \tag{A12}$$

In the weak-coupling limit $x \to \infty$, the oscillator wells become very deep, and the ground-state wave function develops sharp Gaussian peaks like δ functions at the bottom of the wells. This "local" structure will be the same for the lowest states in both the vacuum sector and the axial string sectors. The difference in energy will come from their dependence on the *zero-momentum* angular variables $\tilde{\theta}(0,\hat{\mathbf{i}})$. There is no "potential well" in these variables, and the wave function remains an eigenfunction of $\tilde{L}^2_{\hat{\mathbf{i}}}(0) = -\partial^2/\partial\tilde{\theta}(0,\hat{\mathbf{i}})^2$ at *all* couplings x.

Referring back to the strong-coupling limit, then, we see that, at $x=0$,

$$|\psi_0\rangle = 1, \tilde{L}^2_{\hat{\mathbf{i}}}(0) \equiv 0 \text{ in the vacuum sector;} \tag{A13}$$

whereas

$$|\psi_s\rangle = \exp\left[i \sum_{n=1}^{M} \theta(n\hat{\mathbf{i}},\hat{\mathbf{i}}) \right], \quad \tilde{L}^2_{\hat{\mathbf{i}}}(0) = 1/M \tag{A14}$$

in the axial string sector with a unit flux string in the $\hat{\mathbf{i}}$ direction. Hence the string tension in the weak-coupling limit is

$$T=\frac{1}{M}(E_s-E_0)\underset{x\to\infty}{\sim}\frac{1}{M^2}\ , \tag{A15}$$

behavior characteristic of a critical point. This behavior is exactly analogous to that of the O(2) Heisenberg spin model in 1+1 dimensions,[39] where the mass gap scales like $1/M$ in the weak-coupling limit.

APPENDIX B: LATTICE RENORMALIZATION

Here we derive the form of the Roomany-Wyld approximant[38] for the β function associated with the string tension. The physical Hamiltonian H_p for the model is actually[32,33]

$$H_p=\frac{g^2H}{2a}\ , \tag{B1}$$

where a is a lattice spacing and H is the dimensionless Hamiltonian of Eq. (21). Following Roomany and Wyld,[38] we imagine the theory to be defined in a box of side $L=Ma$, with periodic boundary conditions, where the length L is fixed. We demand that the physics be the same at each lattice spacing a; and in particular we demand that for two systems with M and M' sites on a side, the string tension, or energy per unit length be the same, i.e.,

$$\frac{M}{L}T_p(g,M)=\frac{M'}{L}T_p(g',M')\ , \tag{B2}$$

where $T_p(g,M)$ is the physical energy per link at coupling g. Since $T_p(g,M)=(g^2/2a)T(g,M)=(g^2M/2L)T(g,M)$, where $T(g,M)$ is the dimensionless string tension of Eq. (3.2), the relation (B2) is equivalent to

$$g^2M^2T(g,M)=g'^2M'^2T(g',M')\ . \tag{B3}$$

This defines an effective renormalization-group transformation $g'=R(g)$. Note that at a critical point or fixed point $g'=g=g^*$, (B3) implies the standard finite-size scaling behavior

$$T(g^*,M)\underset{M\to\infty}{\sim}\frac{\text{const}}{M^2}\ . \tag{B4}$$

The Callan-Symanzik β function is defined by

$$\beta(g)=a\left[\frac{\partial g}{\partial a}\right]\Bigg|_{MT_p=\text{const}}\ . \tag{B5}$$

With L fixed, changes of a are related to changes in $M, da/a=-dM/M$. Setting $MT_p=\text{const}$ we find

$$\left[T_p+M\frac{\partial T_p}{\partial M}\right]dM+M\frac{\partial T_p}{\partial M}dg=0 \tag{B6}$$

and hence

$$\frac{\beta(g)}{g}=\left[T_p+M\frac{\partial T_p}{\partial M}\right]\Big/g\frac{\partial T_p}{\partial g} \tag{B6a}$$

$$=\frac{\partial\ln(MT_p)}{\partial\ln M}\Big/\frac{\partial\ln T_p}{\partial\ln g} \tag{B6b}$$

$$=\frac{\partial\ln[M^2T]}{\partial\ln M}\Big/\frac{\partial\ln[Mg^2T]}{\partial\ln g} \tag{B6c}$$

$$=\frac{\ln[M'^2T(g,M')/M^2T(g,M)]}{\ln(M'/M)}\Big/\left[2+\frac{1}{2}g\frac{\partial}{\partial g}\ln[T(g,M)T(g,M')]\right] \tag{B6d}$$

where (B6d) is obtained by approximating the derivative in $\ln M$ by a finite difference. In terms of the variable $x=1/g^4$,

$$\frac{\beta(g)}{g}=\frac{\ln[M'^2T(x,M')/M^2T(x,M)]}{\ln(M'/M)}\Big/2\left[1-x\frac{\partial}{\partial x}\ln[T(x,M)T(x,M')]\right]\ . \tag{B7}$$

Essentially this result was first obtained by Irving and Hamer,[28] but the detailed derivation was not given there. The bulk limit of the β function when $M,M'\to\infty, T(x,M)\to T(x)$, is

$$\frac{\beta(g)}{g}=\frac{1}{1-2x\dfrac{\partial}{\partial x}\ln T}\ , \tag{B8}$$

so that in the case of a second-order phase transition

$$T(x)\underset{x\to x^*}{\sim}(x^*-x)^{\mu}\ , \tag{B9}$$

the β function behaves as

$$\frac{\beta(g)}{g}\underset{x\to x^*}{\sim}\frac{x^*-x}{2\mu x^*}\ , \tag{B10}$$

where μ is the critical index, which can thus be found from the slope of the β function at the critical point.

[1]K. G. Wilson, Phys. Rev. D **10**, 2445 (1974).
[2]A. M. Polyakov, Phys. Lett. **59B**, 82 (1975).
[3]T. Banks, R. Myerson, and J. Kogut, Nucl. Phys. **B129**, 493 (1977); R. Savit, Phys. Rev. Lett. **39**, 55 (1977); S. D. Drell, H. R. Quinn, B. Svetitsky, and M. Weinstein, Phys. Rev. D **19**, 619 (1979).
[4]A. Guth, Phys. Rev. D **21**, 2291 (1980).
[5]J. Fröhlich and T. Spencer, Commun. Math. Phys. **83**, 411 (1982).
[6]J. S. Barber, R. E. Schrock, and R. Schrader, Phys. Lett. **152B**, 221 (1985).
[7]J. M. Kosterlitz and D. J. Thouless, J. Phys. C **6**, 1181 (1973).
[8]M. Creutz, L. Jacobs, and C. Rebbi, Phys. Rev. D **20**, 1915 (1979).
[9]B. Lautrup and M. Nauenberg, Phys. Lett. **95B**, 63 (1980).
[10]G. Bhanot, Phys. Rev. D **24**, 461 (1981).
[11]T. A. DeGrand and D. Toussaint, Phys. Rev. D **24**, 466 (1981).
[12]K. J. M. Moriarty, Phys. Rev. D **25**, 2185 (1982).
[13]D. G. Caldi, Nucl. Phys. **B220**, 48 (1983).
[14]T. Jersak, T. Neuhaus, and P. M. Zerwas, Phys. Lett. **133B**, 103 (1983); Nucl. Phys. **B251**, 299 (1985).
[15]H. G. Evertz, T. Jersak, T. Neuhaus, and P. M. Zerwas, Nucl. Phys. **B251**, 279 (1985).
[16]R. Gupta, M. A. Novotny, and R. Cordery, Phys. Lett. B **172**, 86 (1986).
[17]V. Grösch, K. Jansen, T. Jersak, C. B. Lang, T. Neuhaus, and C. Rebbi, Phys. Lett. **162B**, 171 (1985).
[18]A. N. Burkitt, Nucl. Phys. **B270**, 575 (1986).
[19]C. B. Lang, Nucl. Phys. **B280**, 255 (1987).
[20]A. Hasenfratz, Phys. Lett. B **201**, 492 (1988).
[21]V. Azcoiti, G. DiCarlo, and A. F. Grillo, Phys. Lett. B **238**, 355 (1990).
[22]J. Kogut, D. K. Sinclair, and L. Susskind, Nucl. Phys. **B114**, 199 (1976).
[23]H. W. Hamber, Phys. Rev. D **24**, 941 (1981).
[24]D. W. Heys and D. R. Stump, Nucl. Phys. **B257**, 19 (1985).
[25]D. W. Heys and D. R. Stump, Phys. Rev. D **28**, 2067 (1983); **30**, 1315 (1984).
[26]S. A. Chin, J. W. Negele, and S. E. Koonin, Ann. Phys. (N.Y.) **157**, 140 (1984).
[27]S. E. Koonin, E. A. Umland, and M. R. Zirnbauer, Phys. Rev. D **33**, 1795 (1986).
[28]A. C. Irving and C. J. Hamer, Nucl. Phys. **B235**, 358 (1984).
[29]J. -W. Choe, A. Duncan, and R. Roskies, Phys. Rev. D **37**, 472 (1988).
[30]C. R. Allton, C. M. Yung, and C. J. Hamer, Phys. Rev. D **39**, 3772 (1989).
[31]C. J. Hamer and J. Court, Phys. Rev. D **42**, 2835 (1990).
[32]J. B. Kogut *et al.*, Phys. Rev. D **23**, 2945 (1981).
[33]A. C. Irving, J. F. Owens, and C. J. Hamer, Phys. Rev. D **28**, 2059 (1983).
[34]M. P. Nightingale and H. W. J. Blöte, Phys. Rev. B **33**, 659 (1986).
[35]T. A. DeGrand and J. Potvin, Phys. Rev. D **31**, 871 (1985).
[36]K. Binder, in *Phase Transitions and Critical Phenomena*, edited by C. Domb and M. S. Green (Academic, New York, 1976), Vol. 5b.
[37]T. Hofsäss and R. Horsley, Phys. Lett. **123B**, 65 (1983).
[38]H. Roomany and H. W. Wyld, Phys. Rev. D **21**, 3341 (1980).
[39]C. J. Hamer and M. N. Barber, J. Phys. A **14**, 259 (1981).